Progress In Electromagnetics Research C, Vol. 109, 111–123, 2021

A Novel Wideband Beam Reconfigurable Magneto-Electric Dipole Patch Antenna

Min Wang[1], Huifeng Yang[1], Nan Hu[2], Wenqing Xie[2], Yuxin Mo[1], Zhenghan Chen[1], Zhongyuan Liu[1], and Zhengchuan Chen[3, *]

Abstract—A novel wideband beam reconfigurable magneto-electric dipole patch antenna is presented in this paper. The proposed antenna consists of two H-shaped patches, two folded patches, an E-shaped feeding structure, a side-slotted ground, and a large reflective ground. Two H-shaped patches are horizontally placed on both sides of the feed structure, and two folded patches are assembled vertically to the upper ground, which are designed as the magneto-electric dipole structure. Two symmetrically sided slots are etched on the upper ground to reduce the profile, and an E-shaped strip is employed in the feeding structure to broaden the bandwidth. To suppress the backward radiation, a lower ground with large size is designed as a reflector. Four binary switches are symmetrically integrated on the stubs of H-shaped patches. By switching them ON or OFF simultaneously, the current distribution is changed to achieve beam reconfigurability. Finally, a set of antenna prototype with four configurations is fabricated and measured. The measured results show that maximum impedance bandwidth achieves up to 77.8% at 2.7 GHz from 2.0 GHz to 4.1 GHz. At 2.7 GHz, the measured peak gains are 8.4 dBi, 9.3 dBi, 8.1 dBi, and 8.7 dBi, where the beams point to $-21°$, $0°$, $21°$, and $34°$, respectively in E-plane.

1. INTRODUCTION

Modern wireless communications suffer from the increase in interference between users or electronic jamming. One of the means to resolve the problems is to use a reconfigurable antenna whose characteristics can be reconfigured in terms of frequency, polarization, and radiation beam. Beam reconfigurable antennas have attracted great interest owing to their advantages to transmit/receive signals with flexible direction. These antennas can increase the spectrum utilization by dynamically adjusting their radiation characteristics to the system requirements and the surrounding environment, reducing the cost and space of installation efficiently. In these mobile systems, antennas are desired to dynamically changing their radiation beams in response to variations in traffic distribution. It can improve the capacity efficiency and signal-to-noise-ratio (SNR) of systems.

Beam reconfigurable antenna can generate different radiation patterns on a physical aperture, as shown in Figure 1. In recent years, three beam-steering techniques have been used to design beam reconfigurable antennas: mechanical devices [1, 2], tunable materials [3, 4], and solid state devices, such as PIN diodes [5, 6], varactors [7, 8], and microelectromechanical systems (MEMS) [9]. Mechanical devices have special requirements for structure design where it need be mounted beneath the ground plane to isolate the antenna radiation. Tunable materials are inserted into the substrate of antenna to make it difficult to control the radiation performance of the antenna element independently. As for the solid state devices, they are integrated on the surface of each element to directly involve in the element

Received 28 November 2020, Accepted 26 January 2021, Scheduled 1 February 2021

* Corresponding author: Zhengchuan Chen (czc@cqu.edu.cn).

[1] School of Optoelectronic Engineering, Chongqing University of Posts and Telecommunications, China. [2] A-INFO Inc., Beijing 100084, China. [3] The Key Laboratory of Dependable Service Computing in Cyber-Physical Society, Ministry of Education, and the School of Microelectronics and Communication Engineering, Chongqing University, China.

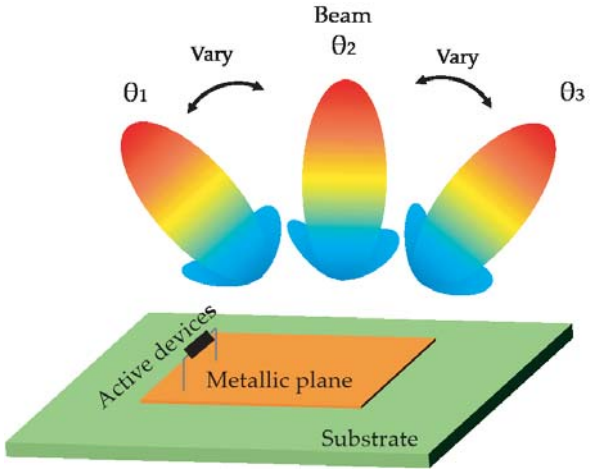

Figure 1. Schematic view of a beam reconfigurable antenna and its integration with active device.

radiation to obtain fast response time. Compared with the former two methods, solid state devices have flexible control characteristics on antenna radiation.

In the literature, a planar microstrip antenna with a single element or several radiating elements is usually designed by integrating active devices to achieve beam reconfiguration [10–12]. This type has disadvantages of low gain or narrow bandwidth, even the limited beam reconfigurable capabilities. Although the antenna gain can be improved quickly by increasing the number of elements [13, 14], the complexity of the feed network or the size of the antenna aperture increases, even the transmission loss of feed network is also increased. By adding artificial electromagnetic surface on the upper or lower space of antenna aperture, the radiation gain can be greatly improved [15, 16]. However, its bandwidth is narrow for the limitation of resonance conditions. Due to the ability to simultaneously excite electric dipole and magnetic dipole with good radiation pattern, magneto-electric (ME) dipole antennas have attracted much attention. By switching active devices loaded on the dipole structure of ME dipole antennas, reconfigurable ME dipole antennas with various flexible radiation capabilities can be achieved, such as beam [17, 18], beamwidth [19, 20], polarization [21, 22], or frequency diversities [23]. On the whole, the research on beam reconfigurable ME dipole antenna is very limited. Among existing designs [17, 18], the gain and bandwidth of the beam reconfigurable ME dipole antenna prototype are insufficient for promotion on application.

To address above challenges, a novel linearly polarized metal-only beam reconfigurable ME dipole patch antenna is presented in this work. The ME dipole radiating structure with four configurations is designed to verify the feasibility of beam reconfigurability. Then, an E-shaped feeding structure is adopted to provide RF energy to obtain a wide impedance bandwidth. To reduce the vertical height of the magnetic dipole structure, a short ground plane with slot etching is designed above the other large ground plane. This paper is organized as follows. The antenna design is presented in Section 2, and parameter analysis is presented in Section 3. Then, the measured results of proposed antenna are shown in Section 4. Finally, the conclusion is given in Section 5.

2. ANTENNA DESIGN

Figure 2(a) shows the design structure of the proposed ME dipole patch antenna. The center frequency is designed at 2.7 GHz, and the polarization is linear along with y-axis. The antenna consists of two horizontally symmetrically placed H-shaped patches as the electric dipole structure, and two vertically folded patches as the magnetic dipole structure, as shown in Figures 2(b) and 2(c). Two pairs of symmetrical rectangles are slotted on the two arms of the electric dipole. To improve the impedance bandwidth, the feeding structure is modified with an E-shaped strip. It consists of two parts, a transmission line with three parallel branches and a coupling strip that is composed of a horizontal rectangular part. Meanwhile, a vertical metallic probe with a radius R of 4.5 mm is used to connect the coupling strip and the inner conductor of the SubMiniature version A (SMA) connector.

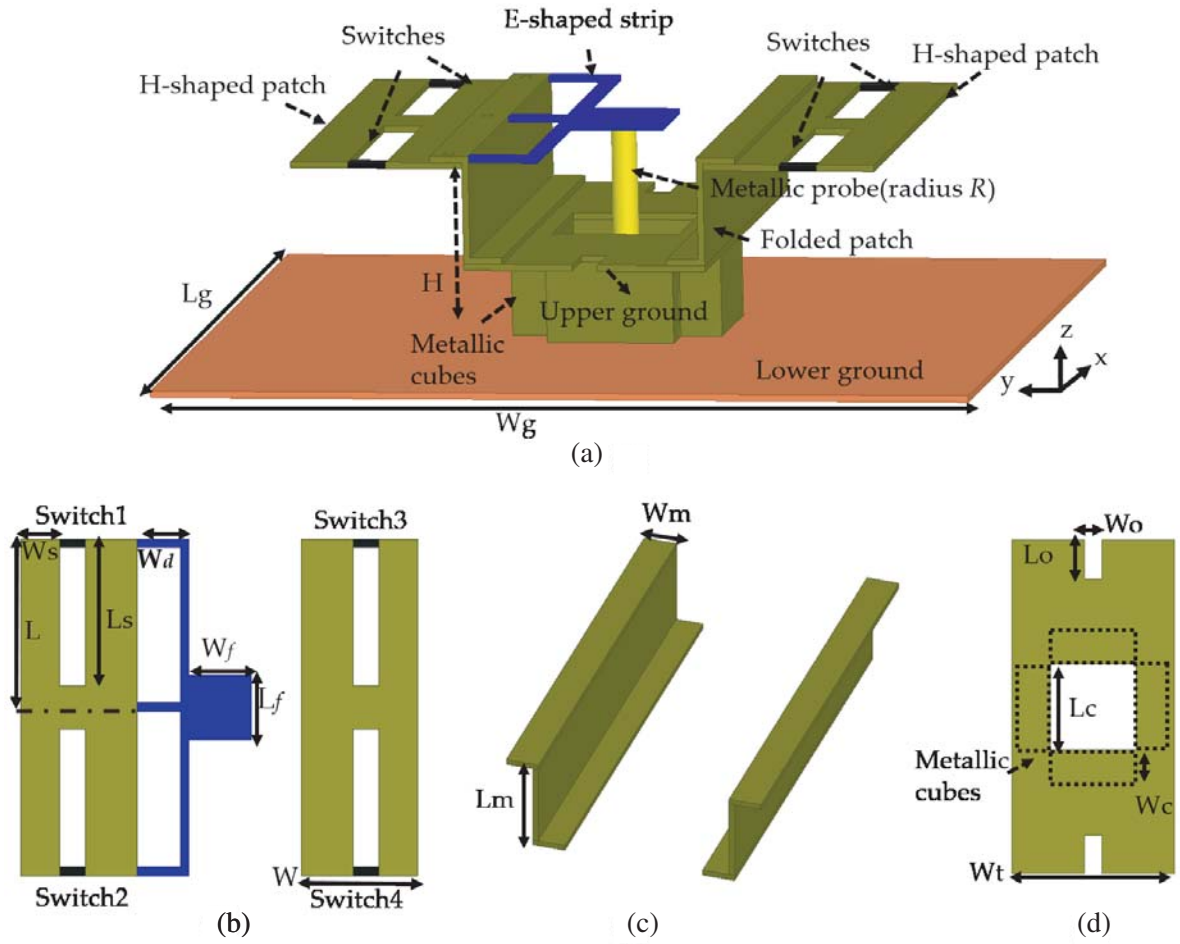

Figure 2. The geometry of proposed antenna. (a) Perspective view of the whole antenna. (b) Two H-shaped patches with E-shaped feeding structure. (c) Two folded patches. (d) Side-slotted upper ground.

The ground is divided into two parts, lower ground as a large reflector, which is used to suppress the backward radiation, and upper ground as a short wall of magnetic dipole antenna. To connect the upper and lower grounds, four metallic cubes with a height of 7 mm ($0.063\lambda_o$) constitute a supporting structure with a square hole ($L_c \times L_c$) in Figure 2(d). Therefore, the input energy is first fed by the SMA to the vertical metallic probe. Then, it transmits along the E-shape strip to horizontal patches and vertical patches for good radiation. To achieve the beam reconfiguration, four binary switches (Switch1, Switch2, Switch3, and Switch4) are loaded on the slots of horizontal H-shaped patches. By selecting ON or OFF state of each switch, four different configurations can operate in the required frequency band, as presented in Table 1 and Figure 3. For simplicity [9, 24, 25], the "ON" state indicates that the slot is short, where two stubs of the H-shaped patch are connected by a metallic line, and the "OFF" state indicates that the slot is open, where the two stubs of the H-shaped patch are disconnected. The metallic sheet used in the antenna is made of stainless steel with a thickness of 1 mm. Some key geometrical parameters are optimized as in Table 2.

The proposed beam reconfigurable metal-only ME dipole patch antenna is analyzed using high frequency structure simulator (HFSS) based on the finite-element method. Radiation boundary condition is applied to the antenna to mimic a free-space environment. Lumped port with 50 ohm input impedance is set as excitation. For explaining the beam reconfiguration operated at four states, the simulated current distributions on the surfaces of the horizontal patches are shown in Figure 4. The lengths of the arms of the electric dipole antenna are controlled using four binary switches, and the

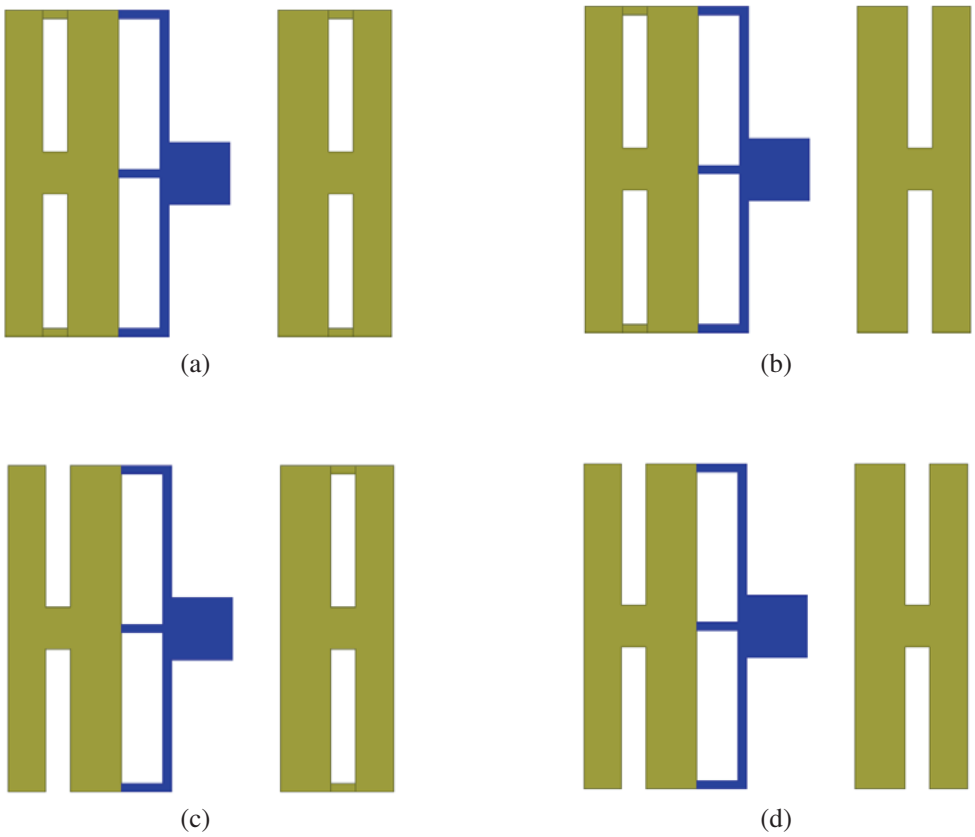

Figure 3. The configurations of four states. (a) State 1. (b) State 2. (c) State3. (d) State4.

Table 1. The states of the proposed antenna.

State	Switch1	Switch2	Switch3	Switch4
1	ON	ON	ON	ON
2	ON	ON	OFF	OFF
3	OFF	OFF	ON	ON
4	OFF	OFF	OFF	OFF

Table 2. The key geometrical parameters of the proposed antenna.

Parameters	L	W	H	L_g	W_g	L_s
Value (mm)	39	28	23	129	129	34
Parameters	W_s	W_d	W_f	L_f	L_o	W_o
Value (mm)	9	11	13	19	9	4
Parameters	W_t	L_m	W_m	W_c	L_c	
Value (mm)	28	16	6	6.5	15	

current distribution varies with the length. Consequently, the dipole shifts the overall radiation beam of the antenna to the direction where the current intensity is stronger. As a result, four different radiation beams can be reconfigured by employing four switches integrated on the arms of electric dipole antenna.

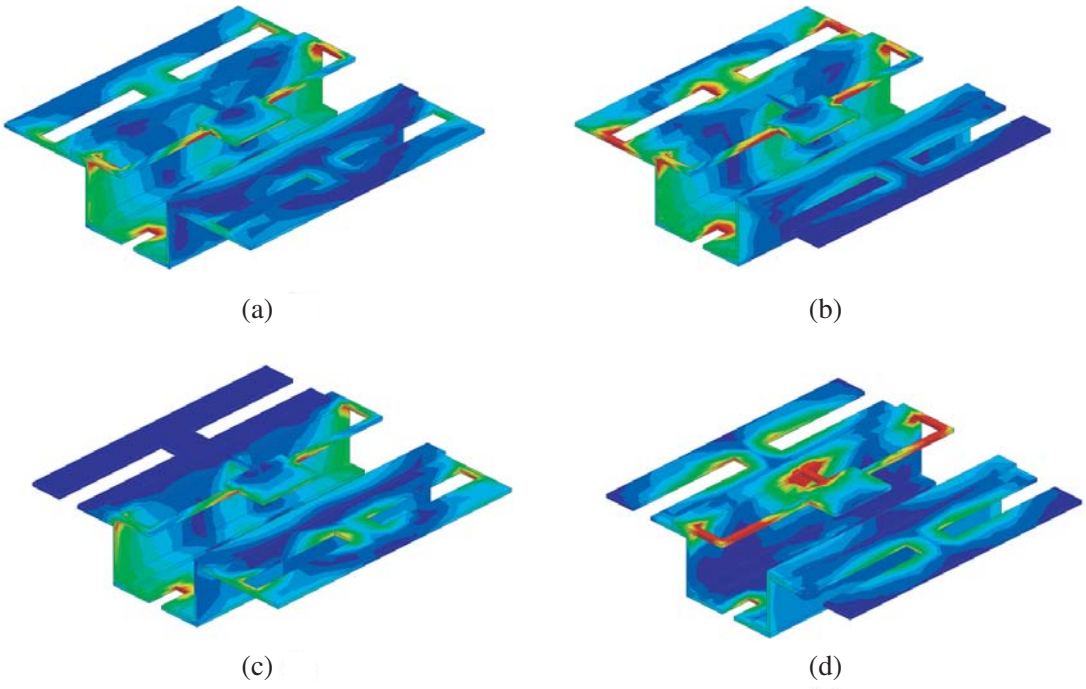

Figure 4. The current distribution of the four states. (a) State 1. (b) State 2. (c) State 3. (d) State 4.

To investigate the working mechanism of the antenna, the reflection magnitude and radiation beams of proposed antenna at four states are studied. As shown in Figure 5, the proposed beam reconfigurable antenna attains its wide bandwidth at four states, where the −10 dB impedance bandwidth covers 2.2 GHz–4.1 GHz at State 1, 2.1 GHz–4.1 GHz at State 2, 2.3 GHz–4.0 GHz at State 3, and 2.3 GHz–4.1 GHz at State 4. The simulated maximum relative bandwidth is up to 74.1% at 2.7 GHz at State 2. For these four states, the overlapped −10 dB impedance band of the proposed antenna covers 2.3 GHz–4.0 GHz. In Figure 6, the radiation beams at four states are designed to switch among four different directions at desired frequency band. The simulated radiation patterns have the performance of high gain, where the gains vary from 7.8 dBi to 9.9 dBi when the display frequencies are 2.5 GHz, 2.7 GHz, and 2.9 GHz. Especially at 2.7 GHz, the radiation beams at State 1, State 2, State 3, and State 4 point to 20°, 33°, −23°, and −1° in E-plane, respectively. The corresponding peak gains at 2.7 GHz

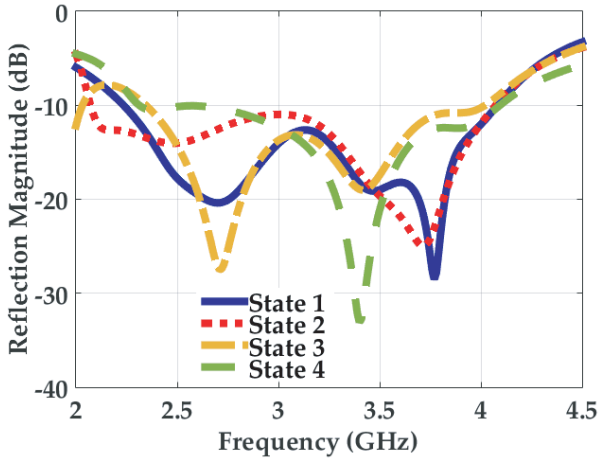

Figure 5. Simulated reflection magnitude versus frequency under four states.

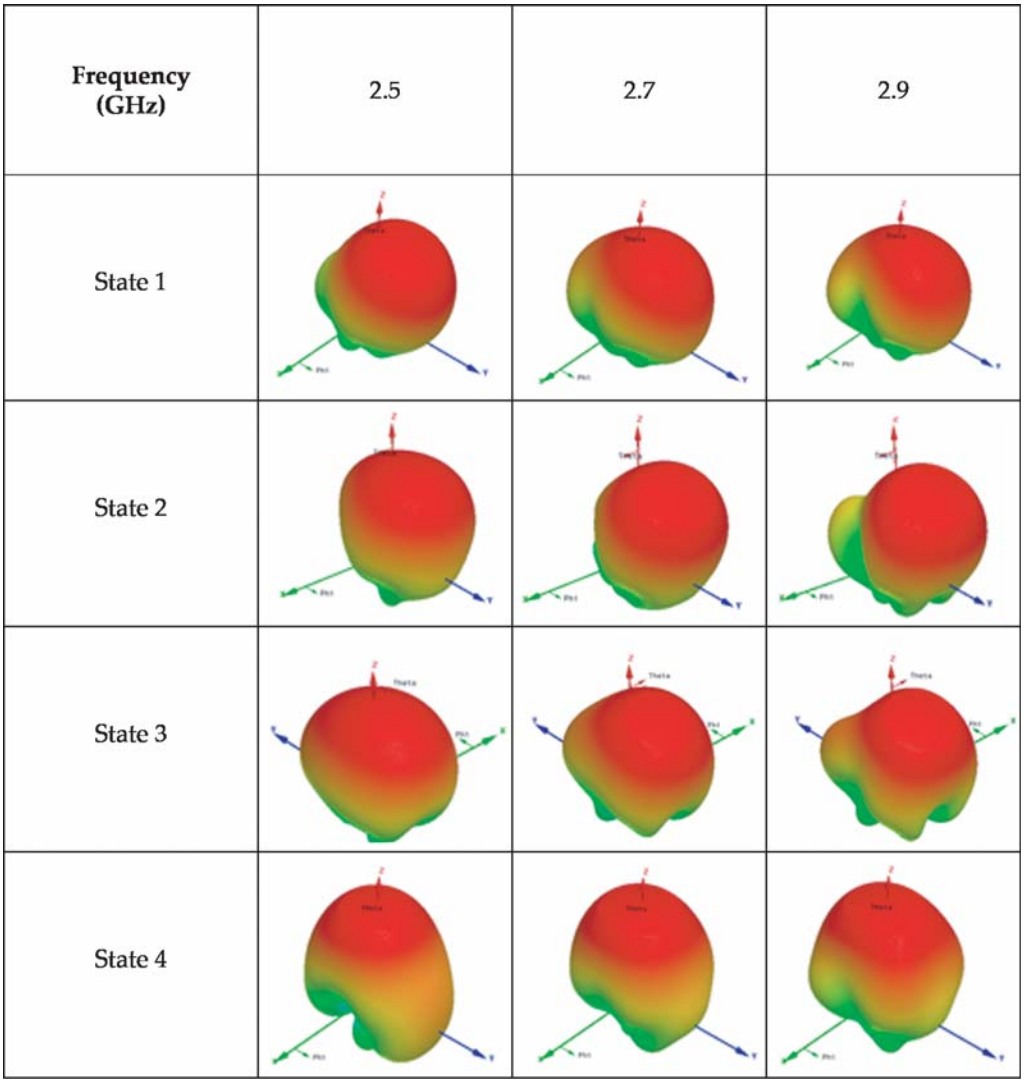

Figure 6. Simulated 3D radiation beams at 2.5 GHz, 2.7 GHz and 2.9 GHz under four states.

are 8.7 dBi, 9.4 dBi, 9.1 dBi, and 9.9 dBi. Although the electric dipole structure of State 2 and State 3 are symmetric, the radiation patterns at State 2 and State 3 are asymmetric. It is caused by the asymmetrical feeding structure.

3. PARAMETER ANALYSIS

Three critical parameters are selected to discuss the influence on the antenna performance. First, the influence of two sided slots etched on the upper ground is described in Figure 7. The simulated current distribution on the surface of non side-slotted ground is shown in Figure 7(a), and the simulated current distribution on the surface of side-slotted ground, where two rectangular slots are etched symmetrically on the edge of the upper ground, is shown in Figure 7(b). Compared with the non side-slotted ground, these two slots increase the effective length of surface current flowing along the outer edge of upper ground to reduce the profile. The profile of the whole antenna is optimized to 23 mm ($0.207\lambda_o$) where the height of the magnetic dipole can be significantly reduced to $0.144\lambda_o$. It is worth mentioning that the height of proposed magnetic dipole structure is 42.4% smaller than $0.25\lambda_o$ in the conventional magnetic dipole structure [18–21]. To obtain a good impedance matching, the length L_o of two sided slots is selected as 9 mm.

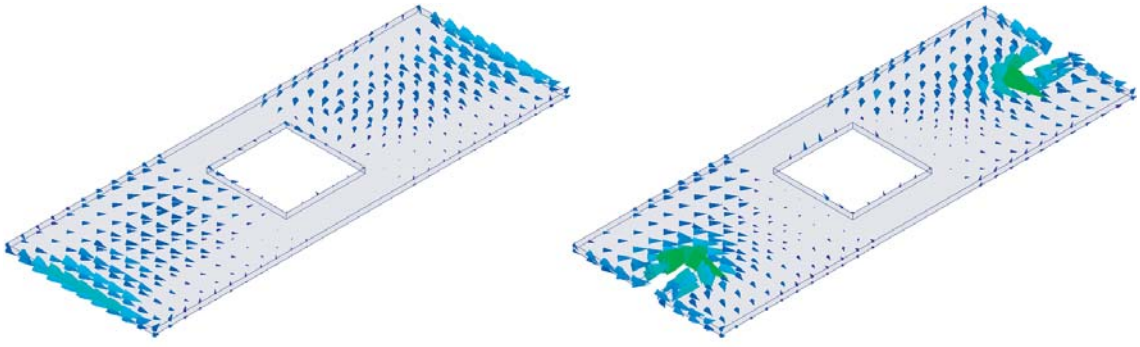

(a) (b)

Figure 7. The current distribution of upper ground at 2.7 GHz under State 1. (a) Non side-slotted ground. (b) Side-slotted ground.

The simulated impedance performance on different radii R of the metallic probe at State 1 is given in Figure 8. The results show that the real part and imaginary part of the input impedance vary with the variation of radius R. As a part of the inner conductor of coaxial connector, the real part of the impedance of the vertical metallic probe decreases with the increase of radius R, which can be derived

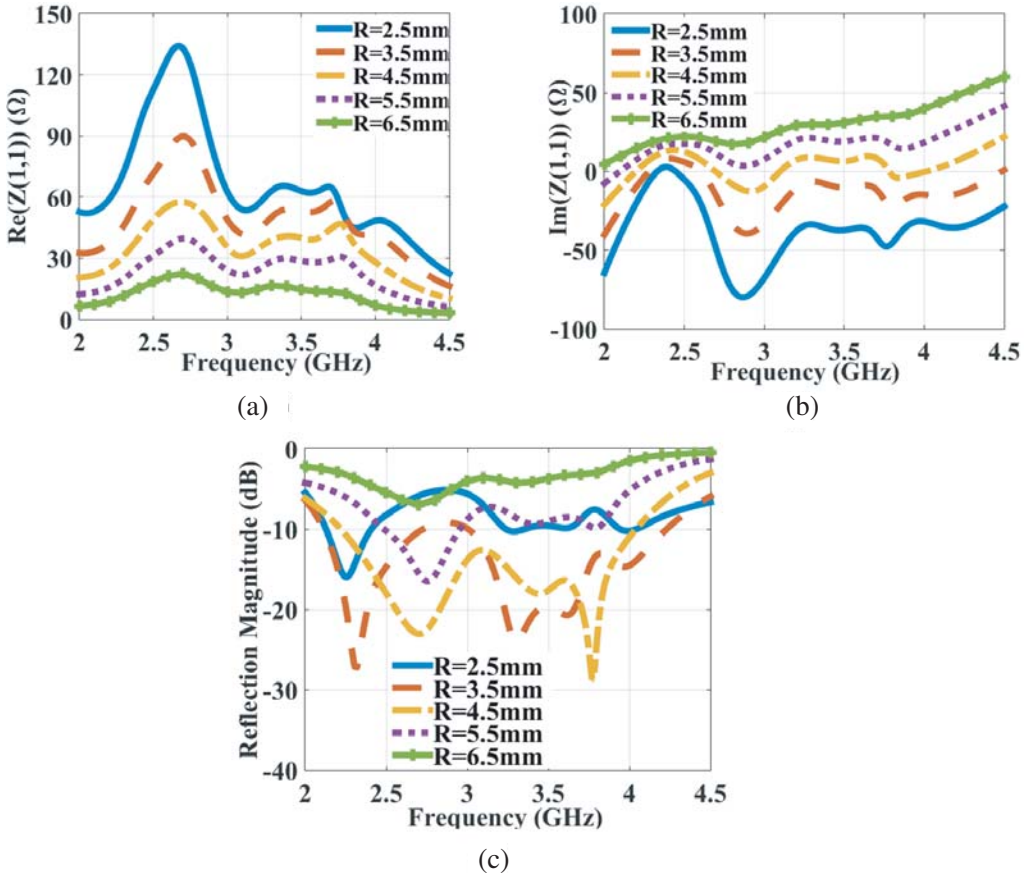

Figure 8. Simulated impedance of different radius R under State 1. (a) Real part. (b) Imaginary part. (c) Reflection magnitude.

from the model of coaxial line as Equation (1):

$$Z_c = \frac{60}{\sqrt{\epsilon_r}} \ln \frac{D}{2R}. \tag{1}$$

In Eq. (1), ϵ_r signifies the relative dielectric constant of the substrate, D the diameter of the outer conductor, and R the radius of the inner conductor. In addition, the vertical metallic probe and the surrounding metallic sheet can be considered as a capacitor. According to the calculation Equation (2) of capacitance derived from cylindrical capacitor:

$$C = \frac{2\pi\epsilon L}{\ln \frac{D}{2R}}. \tag{2}$$

In Eq. (2), ϵ signifies the dielectric constant of the substrate, and L signifies the capacitor length. Referring to Eq. (2) and the negative inversely-proportional relationship between the capacitive impedance and capacitance, it can be judged that the imaginary part of input impedance increases with the increase of the radius R of the inner conductor. Finally, the simulated results verify that with the increase of R, the real part of the input impedance under State 1 decreases, and the imaginary part increases, as shown in Figures 8(a) and 8(b). Therefore, $R = 4.5$ mm is selected to effectively optimize the input impedance of the antenna, thus improving bandwidth of the antenna, as shown in Figure 8(c).

A novel feeding structure with an E-shaped strip is designed to improve the impedance matching of the proposed antenna. The current distributions of I-shaped feeding strip and E-shaped feeding strip are shown in Figure 9(a) and Figure 9(b), respectively. Compared with the conventional feeding design with the I-shaped strip, the E-shaped feeding strip increases two additional branches to achieve different current distributions. It gives more degrees of freedom on the optimization of the impedance to achieve wideband performance. It can be observed from the curves in Figures 10(a) and 10(b) that the E-shaped feeding structure effectively alters the real part and imaginary part of impedance in the frequency band. The E-shaped strip structure works as a capacitive reactance to balance the reactive and resistive parts of impedance produced by the vertical probe and dipole. It should be noted that the length L of I-shaped structure is set as 39 mm for comparison in Figure 10. To achieve better impedance characteristics, the length L is properly optimized as 39 mm, where the maximum bandwidth of 70.4% at State 1 is achieved in Figure 10(c). Of course, the optimized length $L = 39$ mm is finally used as a measured parameter for the proposed E-shaped structure. For the sake of brevity, the analysis of other states, including State 2, State 3, and State 4, is omitted.

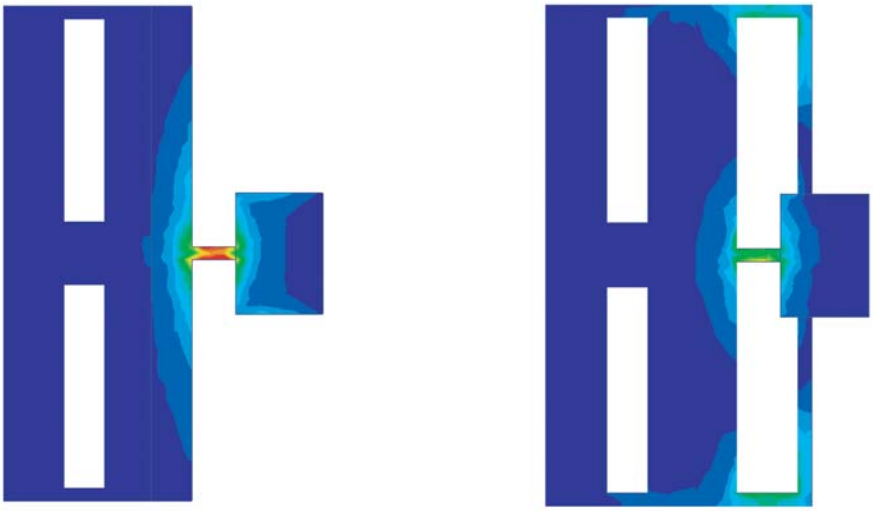

Figure 9. The current distribution of feeding structure at 2.7 GHz under State 1. (a) I-shaped feeding strip. (b) E-shaped feeding strip.

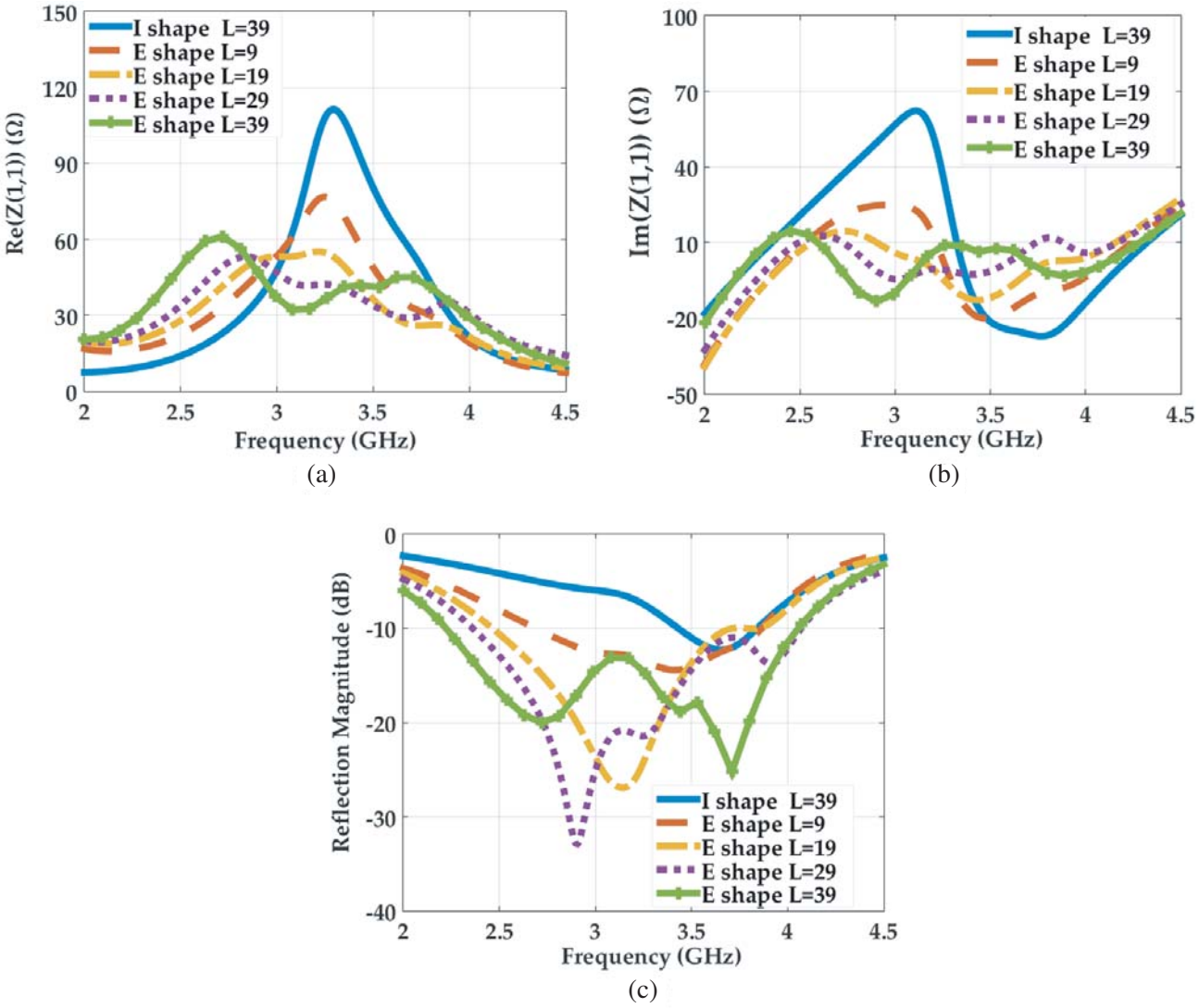

Figure 10. Simulated impedance of feeding structure under State 1. (a) Real part. (b) Imaginary part. (c) Reflection magnitude.

4. MEASURED PERFORMANCE OF PROTOTYPE ANTENNA

In this section, a set of antenna prototype with four configurations based on a metallic line is fabricated to verify the concept of design method of beam reconfigurable ME dipole patch antenna, as shown in Figure 11. The radiating aperture of each configuration is $0.738\lambda_o \times 0.702\lambda_o \times 0.207\lambda_o$ (λ_o at 2.7 GHz). The metallic plates are carved on a 1-mm thick stainless steel sheet using laser cutting technology. Then, they are assembled together using metallic bolts with a diameter of 2 mm. Four metallic cubes and the vertical probe are made of stainless steel, which are soldered on the antenna structure. The SMA connector adopted in antenna prototypes is KFD510 with an impedance of 50 ohm to provide the energy.

At each of the four states, the reflection magnitude is measured by vector network analyzer, and the radiation performance is measured by a far-field anechoic chamber. Figure 12(a) gives the measured reflection magnitude at four states. The measured -10 dB impedance bandwidths are 2.3 GHz–4.0 GHz at State 1, 2.0 GHz–4.1 GHz at State 2, 2.0 GHz–3.9 GHz at State 3, and 2.2 GHz–3.7 GHz at State 4, while the maximum relative bandwidth up to 77.8% at 2.7 GHz at State 2 and overlapped frequency

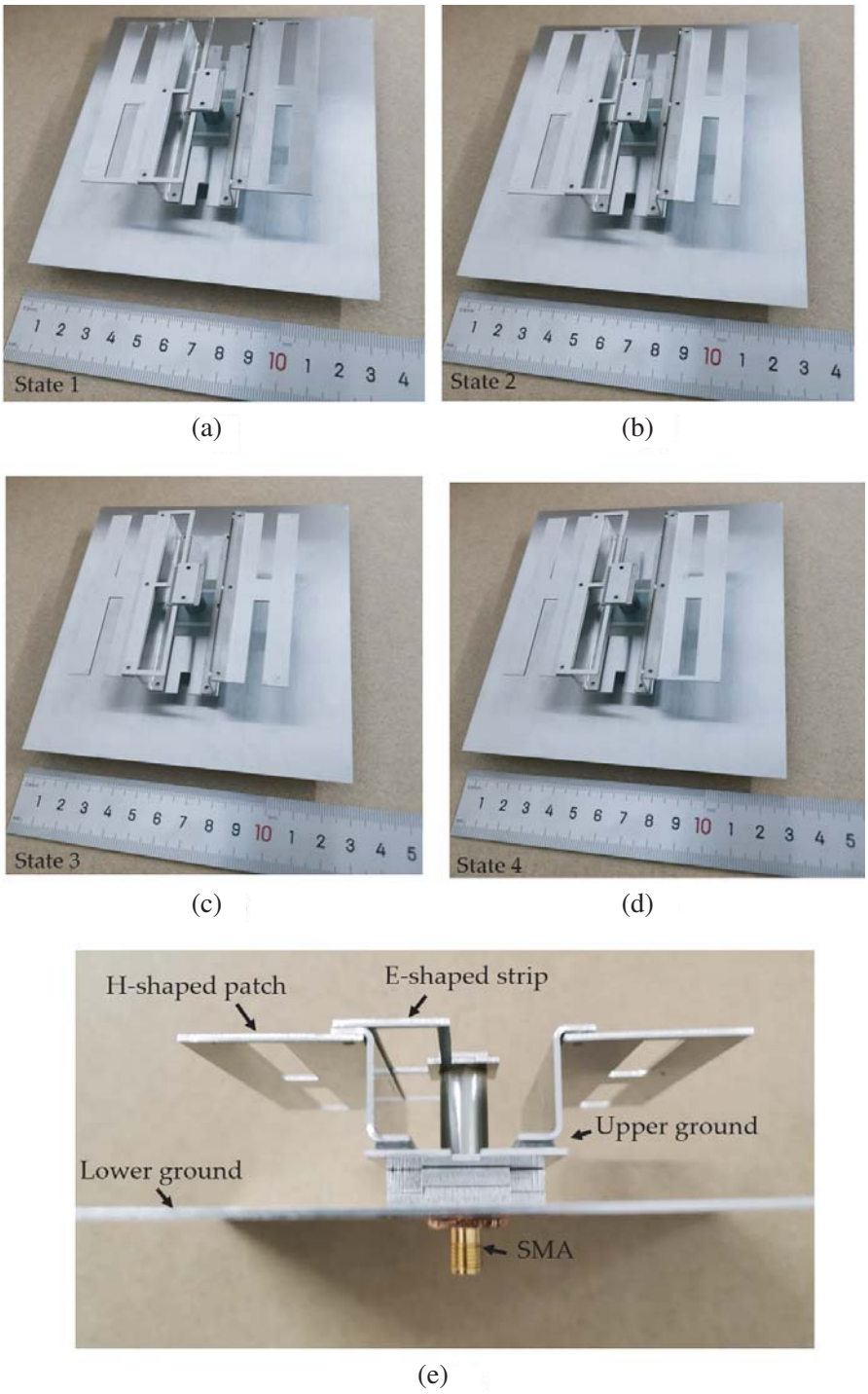

Figure 11. Photographs of prototype antenna with four configurations. (a) State 1. (b) State 2. (c) State 3. (d) State 4. (e) Side view.

band is 2.3 GHz–3.9 GHz. The measured radiation performance at four states is plotted in Figure 12(b). It shows that the prototypes have different beams performance, where the beams point to 21°, 34°, −21°, and 0°, respectively in *E*-plane. The corresponding measured peak gain achieves 8.1 dBi, 8.7 dBi, 8.4 dBi, and 9.3 dBi at 2.7 GHz, with a gain variation of only 1.2 dB at four states. These measured results verify that the proposed design have good performance on bandwidth and beam reconfigurability.

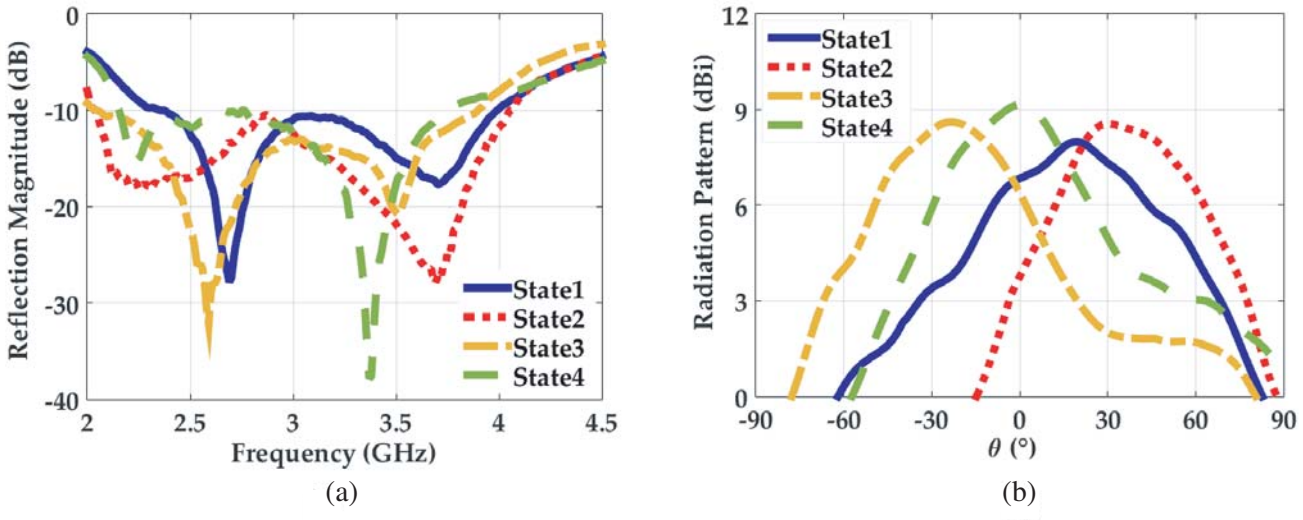

Figure 12. (a) Measured reflection magnitude at four states. (b) Measured radiation beams at 2.7 GHz at four states.

The maximum radiation efficiency corresponding to the measured gain is up to 94% at 2.7 GHz using the following definition:

$$\eta = \text{Gain/Directivity}, \tag{3}$$

where η denotes the radiation efficiency of the antenna.

It has been observed that the measured results at each of the four states are in a reasonable agreement with simulation ones. The discrepancies between them are mainly caused by undesired fabrication inaccuracy and assembly errors. In the process of fabrication and assembly, the size and installation position of the vertical probe have certain deviation. It affects the real part of input impedance, especially at low frequencies, which can be clearly seen in Figure 8(a). Compared with simulated gains at 2.7 GHz, the measured peak gains at four states have a drop about 0.6 dBi–0.7 dBi. The main reason for the decrease in gain is the air gap between metallic sheets in assembly. Besides, the deviation of the measured beam angle is 1° in each state, which is caused by the position error of antenna in the anechoic chamber. As a whole, the discrepancies between simulated and measured results are acceptable.

Table 3. Comparison of Measured Performance in the Literature.

Ref.	Fre. [GHz]	Ant. Type	Beam Direction	Max Gain [dBi]	Max BW [%]
[10]	3.4	AE	−17°, −3°, 0°, 14°	7.3	5.6
[11]	5.8	AE	1°, 26°, 27°	7.5	2.2
[12]	0.8	AE	0°, ±20°	5.0	58.2
[13]	12.2	AA	−60° 60°	22.1	-
[14]	3.5	AA	−52° 52°	17.8	1.5
[15]	5.5	EC	0°, ±22°	10.5	4.5
[16]	5.1	EC	0°, ±6°, ±20°	< 9.0	3.9
[17]	2.4	ME	54°, 66°, 90°	4.3	6.3
[18]	1.3	ME	0°, ±26°	6.2	52.3
This	2.7	ME	±21°, 0°, 34°	9.3	77.8

Note: AE refers to single element antenna, AA refers to array antenna, EC refers to single element antenna using artificial electromagnetic surface. ME refers to magneto-electric dipole antenna.

A comparison of the performance of the proposed antenna with some representative beam reconfigurable designs in the literature is presented in Table 3. The proposed prototypes can point to four different directions by switching four different states, to prove its feasibility in beam reconfigurability of ME dipole antenna. It is obvious that the proposed design method in this work can effectively improve the bandwidth and gain, and reduce the profile.

5. CONCLUSION

As a good candidate for modern wireless communications, beam reconfigurable antenna has attracted growing attention. In this paper, a novel linearly polarized metal-only beam reconfigurable ME dipole patch antenna is presented. A symmetrical side-slotted design is utilized on ground to reduce the profile of a magnetic dipole antenna to $0.144\lambda_o$, and an E-shaped strip as a feeding structure has been proved to be very effective to obtain a wide impedance bandwidth. By selecting the states of switches loaded on the electric dipole, the beam-reconfigurable capability with four different configurations is achieved, where the measured radiation beams point to $-21°$, $0°$, $21°$, and $34°$ in E-plane, and the corresponding gains are 8.4 dBi, 9.3 dBi, 8.1 dBi, and 8.7 dBi at 2.7 GHz. Besides, the maximum impedance bandwidth is up to 77.8%. The simulation and experiment demonstration of the concept is promising for beam reconfigurable ME dipole antenna, and further work should address techniques for the integration of real active device on the proposed antenna prototype.

ACKNOWLEDGMENT

This work was supported in part by the National Natural Science Foundation of China under Grant 62001074, in part by the Chongqing Science and Technology Commission under Grant cstc2020jcyj-msxmX0644 and Grant cstc2019jcyj-msxmX0575, in part by the Scientific and Technological Research Program of Chongqing Municipal Education Commission under Grant KJQN202000642, and in part by the Entrepreneurship and Innovation Support Plan of Chongqing for Returned Overseas Scholars under Grant cx2019105.

REFERENCES

1. Zhu, H. L., S. W. Cheung, and T. I. Yuk, "Mechanically pattern reconfigurable antenna using metasurface," *IET Microw. Antennas. Propag.*, Vol. 9, No. 12, 1331–1336, 2015.
2. Yang, X., S. Xu, F. Yang, M. Li, Y. Hou, S. Jiang, and L. Liu, "A broadband high-efficiency reconfigurable reflectarray antenna using mechanically rotational elements," *IEEE Trans. Antennas Propag.*, Vol. 65, No. 8, 3959–3966, 2017.
3. Erdil, E., K. Topalli, N. S. Esmaeilzad, Ö. Zorlu, H. Kulah, and O. Civi, "Reconfigurable nested ring-split ring transmitarray unit cell employing the element rotation method by microfluidics," *IEEE Trans. Antennas Propag.*, Vol. 63, No. 3, 1163–1167, 2015.
4. Yang, X., Y. Liu, H. Lei, Y. Jia, P. Zhu, and Z. Zhou, "A radiation pattern reconfigurable Fabry-Pérot antenna based on liquid metal," *IEEE Trans. Antennas Propag.*, Vol. 68, No. 11, 7658–7663, 2020.
5. Yang, H., F. Yang, X. Cao, S. Xu, J. Gao, X. Chen, M. Li, and T. Li, "1600-element dual-frequency electronically reconfigurable reflectarray at X/Ku-band," *IEEE Trans. Antennas Propag.*, Vol. 65, No. 6, 3024–3032, 2017.
6. Wang, M., S. Xu, F. Yang, and M. Li, "Design and measurement of a 1-bit reconfigurable transmitarray with subwavelength H-shaped coupling slot elements," *IEEE Trans. Antennas Propag.*, Vol. 67, No. 5, 3500–3504, 2019.
7. Nicholls, J. G. and V. H. Sean, "Full-space electronic beam-steering transmitarray with integrated leaky-wave feed," *IEEE Trans. Antennas Propag.*, Vol. 64, No. 8, 3410–3422, 2016.
8. Frank, M., F. Lurz, R. Weigel, and A. Koelpin, "Electronically reconfigurable 6×6 element transmitarray at K-band based on unit cells with continuous phase range," *IEEE Antennas Wireless Propag. Lett.*, Vol. 18, No. 4, 796–800, 2019.

9. Guclu, C., J. Perruisseau-Carrier, and O. Civi, "Proof of concept of a dual-band circularly-polarized RF MEMS beam-switching reflectarray," *IEEE Trans. Antennas Propag.*, Vol. 60, No. 11, 5451–5455, 2012.
10. Deng, W., X. Yang, C. Shen, J. Zhao, and B. Wang, "A dual-polarized pattern reconfigurable Yagi patch antenna for micro base stations," *IEEE Trans. Antennas Propag.*, Vol. 65, No. 10, 5095–5102, 2017.
11. Ahn, B., H. Jo, J. Yoo, J. Yu, and H. Lee, "Pattern reconfigurable high gain spherical dielectric resonator antenna operating on higher order mode," *IEEE Antennas Wireless Propag. Lett.*, Vol. 18, No. 1, 128–132, 2019.
12. Darvazehban, A., S. Rezaeieh, and A. Abbosh, "Pattern-reconfigurable loopCdipole antenna for electromagnetic pleural effusion detection," *IEEE Trans. Antennas Propag.*, Vol. 68, No. 8, 5955–5964, 2020.
13. Wang, M., S. Xu, F. Yang, N. Hu, W. Xie, and Z. Chen, "A novel 1-bit reconfigurable transmitarray antenna using a C-shaped probe-fed patch element with broadened bandwidth and enhanced efficiency," *IEEE Access*, Vol. 8, 120124–120133, 2020.
14. Zhang, X. G., W. X. Jiang, H. W. Tian, Z. X. Wang, Q. Wang, and T. J. Cui, "Pattern-reconfigurable planar array antenna characterized by digital coding method," *IEEE Trans. Antennas Propag.*, Vol. 68, No. 2, 1170–1175, 2020.
15. Ji, L., Z. Zhang, and N. Liu, "A two-dimensional beam-steering Partially Reflective Surface (PRS) antenna using a reconfigurable FSS structure," *IEEE Antennas Wireless Propag. Lett.*, Vol. 18, No. 6, 1076–1080, 2019.
16. Yang, X., Y. Liu, H. Lei, Y. Jia, P. Zhu, and Z. Zhou, "A radiation pattern reconfigurable Fabry Pérot antenna based on liquid metal," *IEEE Trans. Antennas Propag.*, Vol. 68, No. 11, 7658–7663, 2020.
17. Liang, Z., Z. Liang, Y. Li, J. Liu, J. Qin, and Y. Long, "Reconfigurable microstrip magnetic dipole antenna with switchable conical beams for aerial drone applications," *IEEE Access*, Vol. 7, 31043–31054, 2019.
18. Rezaeieh, S. and A. Abbosh, "Pattern-reconfigurable magnetoelectric antenna utilizing asymmetrical dipole arms," *IEEE Antennas Wireless Propag. Lett.*, Vol. 18, No. 4, 688–692, 2019.
19. Shi, Y., Y. Cai, J. Yang, and L. Li, "A magnetoelectric dipole antenna with beamwidth reconfiguration," *IEEE Antennas Wireless Propag. Lett.*, Vol. 18, No. 4, 621–625, 2019.
20. Ji, Y., L. Ge, J. Wang, Q. Chen, and W. Wu, "Differentially-fed aperture-coupled magneto-electric dipole antenna with continuously variable beamwidth," *IEEE Open J. Antennas Propag.*, Vol. 1, 165–174, 2020.
21. Wu, F. and K. M. Luk, "Single-port reconfigurable magneto-electric dipole antenna with quad-polarization diversity," *IEEE Trans. Antennas Propag.*, Vol. 65, No. 5, 2289–2296, 2017.
22. Gao, S., H. Lin, L. Ge, and D. Zhang, "A magneto-electric dipole antenna with switchable circular polarization," *IEEE Access*, Vol. 7, 40013–40018, 2019.
23. Feng, B., T. Luo, Q. Zeng, and K. L. Chung, "Frequency reconfigurable antenna with triple linear polarisation and wide H-plane characteristic for future smart communications," *IET Microw., Antennas Propag.*, Vol. 12, No. 15, 2276–2284, 2018.
24. Karmokar, D., K. Esselle, and S. Hay, "Fixed-frequency beam steering of microstrip leaky-wave antennas using binary switches," *IEEE Trans. Antennas Propag.*, Vol. 64, No. 6, 2146–2154, 2016.
25. Chang, L., Y. Li, Z. Zhang, and Z. Feng, "Reconfigurable 2-bit fixed-frequency beam steering array based on microstrip line," *IEEE Trans. Antennas Propag.*, Vol. 66, No. 2, 683–691, 2018.